

Targeted disruption of deep-lying neocortical microvessels in rat using ultrashort laser pulses

N. Nishimura^{1,4}, C.B. Schaffer^{1,4}, B. Friedman², P.S. Tsai^{1,4}, P.D. Lyden^{2,3} and D. Kleinfeld^{*1,3,4}

¹Department of Physics, ²Department of Neurosciences, ³Graduate Program in Neuroscience, ⁴Center for Theoretical Biological Physics

University of California at San Diego, La Jolla, CA 92093.

ABSTRACT

The study of neurovascular diseases such as vascular dementia and stroke require novel models of targeted vascular disruption in the brain. We describe a model of microvascular disruption in rat neocortex that uses ultrashort laser pulses to induce localized injury to specific targeted microvessels and uses two-photon microscopy to monitor and guide the photodisruption process. In our method, a train of high-intensity, 100-fs laser pulses is tightly focused into the lumen of a blood vessel within the upper 500 μm of cortex. Photodisruption induced by these laser pulses creates injury to a single vessel located at the focus of the laser, leaving the surrounding tissue intact. This photodisruption results in three modalities of localized vascular injury. At low power, blood plasma extravasation can be induced. The vessel itself remains intact, while serum is extravasated into the intercellular space. Localized ischemia caused by an intravascular clot results when the photodisruption leads to a brief disturbance of the vascular walls that initiates an endogenous clotting cascade. The formation of a localized thrombus stops the blood flow at the location of the photodisruption. A hemorrhage, defined as a large extravasation of blood including plasma and red blood cells, results when higher laser power is used. The targeted vessel does not remain intact.

Keywords: Brain, stroke, nonlinear microscopy, two-photon microscopy, blood flow, hemorrhage, ischemia, ablation, photodisruption, optical breakdown

1. INTRODUCTION

Neurovascular disorders take a heavy toll on the adult population. In addition to fatalities caused by acute problems such as large-scale strokes, chronic disorders such as dementia affect a vast segment of the elderly population. Recently, diffuse neurovascular disruptions, such as small ischemic strokes and leaky vasculature, have been linked with many forms of dementia such as Alzheimer's disease and vascular dementia¹⁻⁴. Microbleeds, or evidence of small hemorrhages detected by magnetic resonance imaging, may be potent indicators of hemorrhage risk during thrombolytic therapy that poses a major complication in treatments for stroke and cardiovascular disease^{5,6}. These diseases are characterized by isolated areas of neuronal death that are thought to be caused by disruption of one or a limited number of vessels. To study the progression of such lesions, a model is needed in which vascular disruptions can be precisely located, while leaving the surrounding tissue sufficiently intact. Since it is not known what type of vascular disturbance is the cause of the neural problems, a model that includes several controllable types of vascular disruption is important. We seek to develop a model of localized, deep-lying vascular disruption that enables the study of the progression of pathology and the effects of potential therapeutics in the neighboring parenchymal tissue.

Photodisruption with ultrashort pulses has proven to be useful for applications that require sub-surface material disruption with micrometer resolution without affecting the surrounding region. The capability of sub-surface machining was first used in transparent solids⁷⁻⁹ and then commercialized for laser eye surgery¹⁰. The precision of the ultrashort photodisruption in biological applications was demonstrated by *in vitro* sub-cellular disruption^{11,12} and by all-optical histology of tissue¹³. Here we extend the advantages of ultrashort laser-induced photodisruption to *in vivo*, three-dimensionally localized disruption of microvasculature deep to the cortical surface. Since several types of vascular insult may lead to neuronal lesions, we develop methods to vary the vascular disruption. Candidates for vascular disturbances we wish to study include (i) extravasation of blood plasma which is toxic to neurons into the parenchymal space, (ii) ischemic insults resulting from the cessation of blood flow in local vessels, and (iii) hemorrhages in which vessels rupture and allow cells in the blood to invade the parenchyma.

* dk@physics.ucsd.edu; phone: 858-882-0342, fax: 858-534-7697; www-physics.ucsd.edu/neurophysics/

We use two-photon laser scanning microscopy (TPLSM) of fluorescently labeled blood plasma to target and monitor the disruption of individual blood vessels¹⁴⁻¹⁶. TPLSM also allows us to observe changes in blood flow resulting from the disruption. The capability to precisely target injury allows the relevant tissue to be located for post-mortem analysis such as immunocytochemistry and histology.

2. METHODOLOGY

2.1 Surgical Preparation

Sprague-Dawley rats (6), 100-300g, were anesthetized with urethane (150mg/100g rat interperitoneal injection) and supplemented as necessary. Atropine sulfate (0.005mg/100g rat) was injected subcutaneously at the beginning of the experiment. Every hour, we supplement with atropine sulfate (0.001mg/100g rat) and with 5% glucose in saline (0.5mL/100g rat). A craniotomy was performed over parietal cortex for optical access. The dura was removed and a metal frame was glued to the skull¹⁷. The exposed brain surface was covered with 1.5% agarose in artificial cerebro-spinal fluid¹⁸. A coverslip was clipped in place on top of the agarose to maintain pressure over the brain. A wide-field image of the entire window was taken with a CCD camera to create a map of surface vasculature. The animal is then transferred to a TPLSM setup modified for simultaneous photodisruption (Fig. 1).

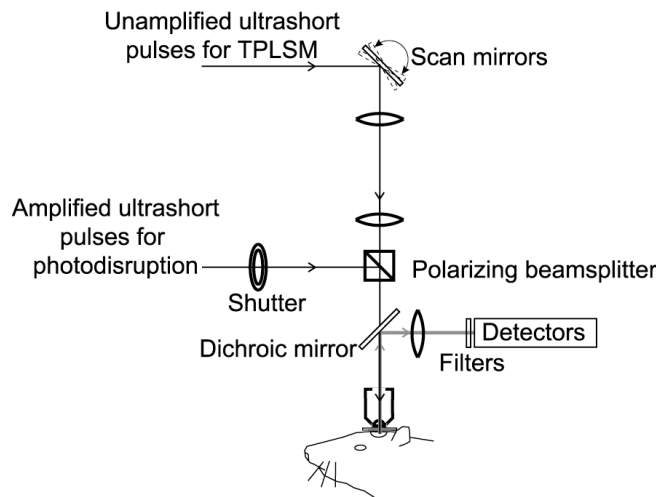


Figure 1. Schematic of two-photon laser scanning microscope (TPLSM) modified for delivery of amplified ultrashort pulses for photodisruption. Unamplified ultrashort pulses for imaging are raster scanned by scan mirrors that are then relay-imaged to the back of a 40x, 0.8-NA, water immersion objective. Two-photon excited fluorescence is collected by a dichroic mirror and photomultiplier tubes. Maximum line-scan rate is 1.3 kHz. Amplified ultrashort pulses for photodisruption are routed through a shutter and to the same objective by a polarizing beamsplitter.

2.2 Two-photon laser scanning microscopy

To visualize the vasculature using TPLSM, fluorescein-isothiocyanate dextran (2 MDa, ~0.3 mL per rat of 5% wt/vol) was injected intravenously to label the blood plasma. The fluorescein labels the plasma, while red blood cells and other solid bodies exclude the fluorescently labeled plasma and appear as dark areas within the lumen of a blood vessel. TPLSM was used in three ways. First, TPLSM was used to monitor the production of the vascular disruptions in real-time with frame scans. Second, z-stacks of TPLSM images spanning the area surrounding the target vessel from the pial surface to ~600 μm below the surface, were obtained before and after photodisruption. Lastly, TPLSM line scans of flow in single vessels were used to quantify red blood cell speed¹⁴.

2.3 Photodisruption of microvasculature

After mapping the vasculature and selecting the target vessel, a train of amplified 1-kHz, 100-fs, 800-nm laser pulses¹⁹ is focused into the lumen of the vessel while we monitored continuously with TPLSM. One of three types of vascular injury is selected by varying the laser pulse energy (0.1 to 10 μJ) and the number of pulses (2 to 10). The laser pulse energy started below the threshold of observed disruption to the vessel, ~0.05 μJ . If no vascular changes were observed, we increased the laser power and repeated irradiation. The actual energy at which vascular

disruption occurred varied in the range of 0.1 to 5 μJ from vessel to vessel, even within the same animal, and depends on the depth of the target. Other factors include scattering, absorption and optical aberrations, which depend strongly on the regional properties of the target vessel; for example, the number, shape and size of the vessels above the target vessel. The lowest energy disruption observable by TPLSM is the extravasation of the fluorescent plasma. Usually, the initial extravasation is produced with ~ 2 pulses and does not result in sufficient thrombosis to impede flow through the vessel. To form an occlusion, the vessel is irradiated with additional bursts of 2-10 pulses at threshold energy. Hemorrhages are induced using higher laser pulse energies.

3. RESULTS

Photodisruption was performed on vessels in the cortex ranging in depth from the surface to $\sim 500 \mu\text{m}$ beneath the surface. The resulting vascular disruptions divide into three categories and are ordered in terms of the approximate severity and size of the damage to the microvessel. In this proceeding we present *in vivo* TPLSM observations of our results.

3.1 Blood plasma extravasation

Following photodisruption, a failure of the blood brain barrier allowed the extravasation of fluorescein-labeled plasma to fill a volume around the targeted vessel (as in Fig. 2). The leakage of plasma appeared to be transient, because the fluorescence outside of the target vessel stabilized within minutes after the irradiation. Penetration of the serum into the extra-vascular space was not limited to regions immediately adjacent to the target vessel. Fluorescent dye penetrated the parenchyma out to $\sim 30 \mu\text{m}$ radially from the target vessel and preferentially followed the along the length of the target vessel. In some instances, leakage through the blood brain barrier was accompanied by thrombosis within the vessel that partially obstructed the vessel. In other cases, blood flow remained unobstructed within the target vessel throughout irradiation, extravasation and subsequent observation (as in Fig. 2).

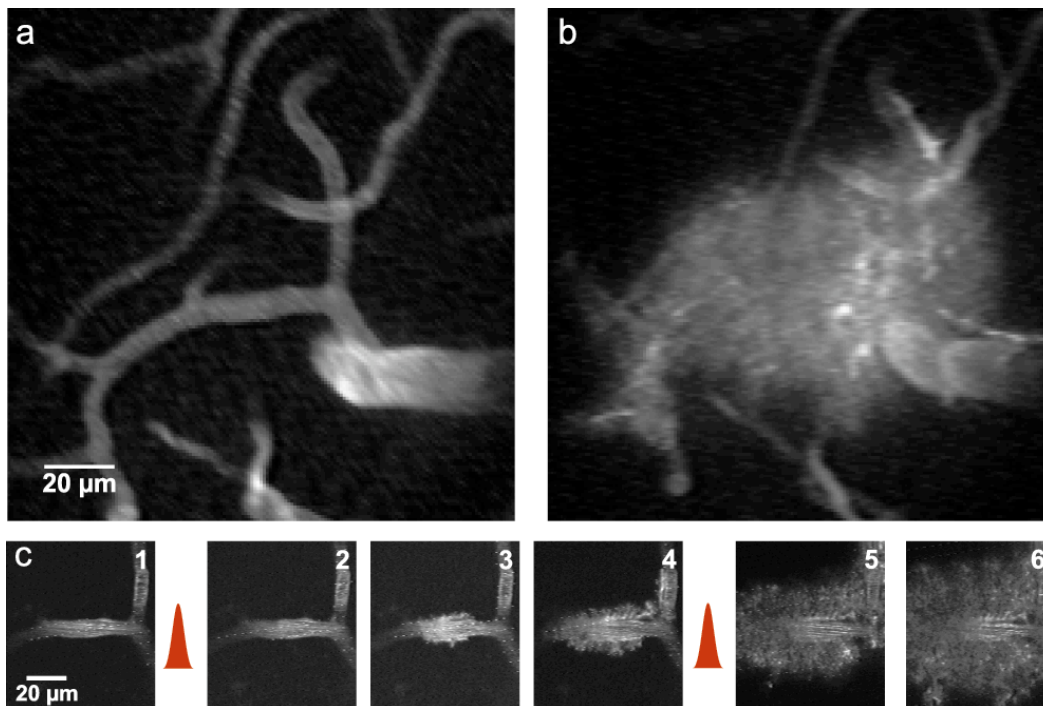


Figure 2. (a) Before and (b) after maximal projections of TPLSM z-stacks of cortical microvessels and blood plasma extravasation induced in the target vessel by ultrashort laser pulses. (c) Time series of TPLSM images during the formation of the plasma extravasation. Irradiation by amplified ultrashort pulses (0.8 μJ) indicated by pulse icons. Streaks visible in the vessel lumens are due to red blood cell motion during the image acquisition and indicate flow. Target vessel was $90 \mu\text{m}$ below the cortical surface.

3.2 Intravascular clot

Repeated irradiation of the target vessel after a blood plasma extravasation can lead to the formation of an intravascular clot. In these cases, thrombosis leads to a complete occlusion of the target vessel, potentially subjecting the surrounding tissue to an ischemic insult. Figure 3c shows a series of TPLSM images from various time points before, during and after the formation of an intravascular clot. Before the irradiation, the vessel was intact. After irradiation with 10 pulses of $0.3 \mu\text{J}$, a small amount of extravasated plasma could be visualized as fluorescence outside the vessel walls. The vessel lumen remained unobstructed. Extravasated fluorescence continued to spread for several seconds after irradiation, but remained spatially confined to within $5 \mu\text{m}$ of the vessel. After a second irradiation with 10 pulses at $0.3 \mu\text{J}$, thrombosis began within several seconds. In the targeted vessel lumen, dark areas indicate the coalescence of red blood cells and perhaps platelets. Bright stationary areas indicate plasma within the vessel that may be stagnant and is without red blood cells. The clot in Fig. 3 was observed to be stable for the entire period of observation (2 hours).

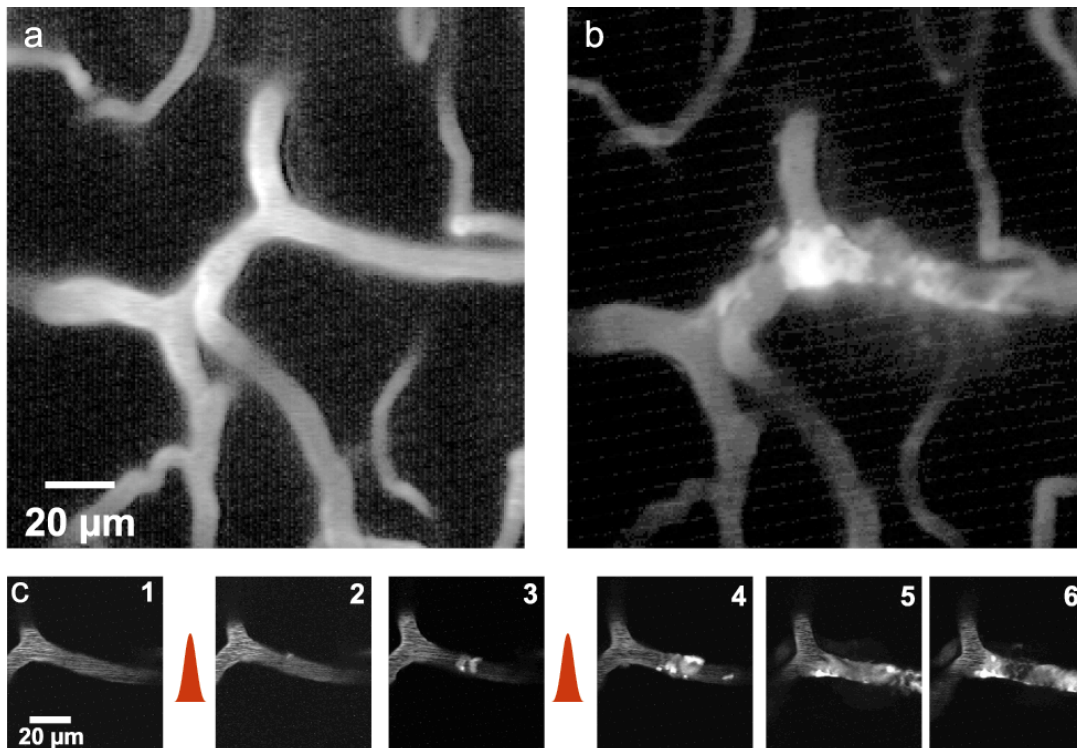


Figure 3. (a) Before and (b) after maximal projections of TPLSM z-stacks of cortical microvessels and induction of an intravascular clot by ultrashort laser pulses. (c) Time series of the formation of the clot. Pulse icon indicates irradiation by amplified ultrashort laser pulses. Target vessel is approximately $150 \mu\text{m}$ below cortical surface.

3.3 Hemorrhage Laser energies in excess of about a factor of 10 above the threshold energy lead to hemorrhage, a larger disruption of the targeted vessel. In Figure 4 a microvessel $125 \mu\text{m}$ below the cortical surface is shown before and after irradiation with 10 pulses of $2 \mu\text{J}$ in energy. Initial fluorescein leakage was rapid, reaching a diameter of $60 \mu\text{m}$ within 1 s. The fluorescent blood plasma continued to expand, stabilizing to a volume of about 0.002 mm^3 . In addition to blood plasma, red blood cells were pushed into the parenchyma and were visualized with white light microscopy immediately after photodisruption. After irradiation, the target vessel was no longer visible, and the darkened, center region was filled with red blood cells, forming a hematoma.

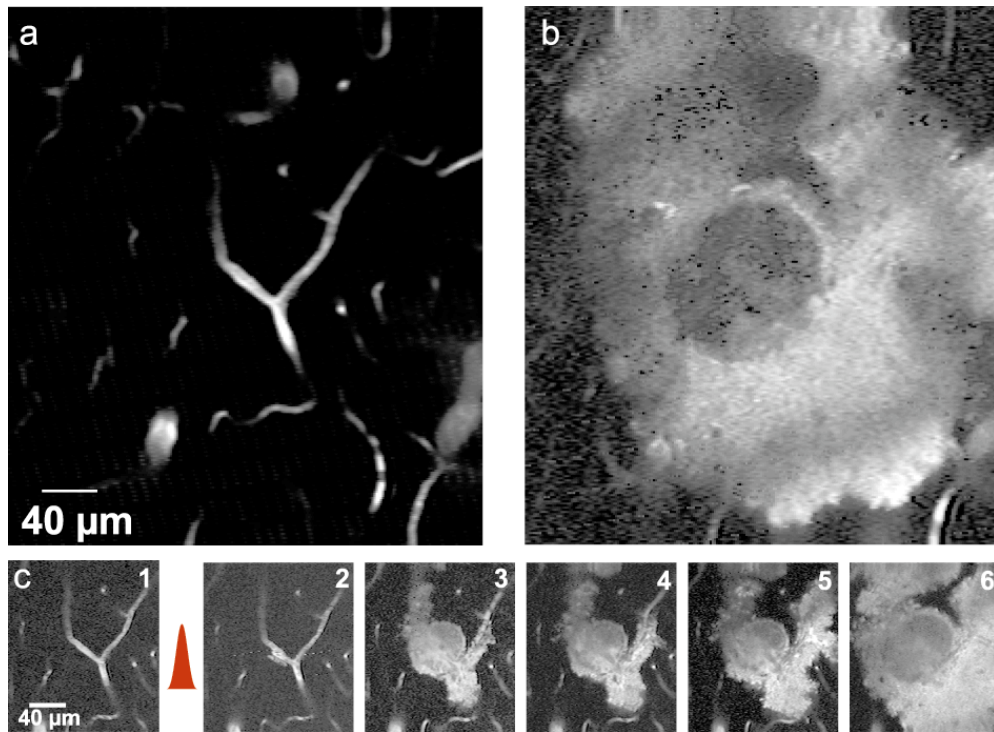


Figure 4. (a) Before and (b) after maximal projections of TPLSM z-stacks of cortical microvessels and formation of a hemorrhage by ultrashort laser pulse irradiation. Dark, circular region in the center is filled with red blood cells. (c) Time series of the formation of the hemorrhage. Fluorescein-labeled plasma and red blood cells invade the surrounding neural tissue.

3. DISCUSSION

We have demonstrated a method for producing injury to single, selected microvessels in the depth of rat cortex using femtosecond laser-induced photodisruption. Our model produces three types of vascular damage shown schematically in Fig. 5: blood plasma extravasation, intravascular clots, and hemorrhage. The thrombotic clotting of single vessels (Fig 3) may be a good model of local blockages of the microvasculature that lead to small areas of ischemia and ultimately, to infarcts in the brain. Local leakage of blood constituents is modeled by the laser-induced blood plasma extravasation (Fig. 2). These insults may mimic the cause of non-ischemic neural damage caused by leaky blood vessels. The sub-surface hemorrhages shown in Fig. 4 will allow the study of interactions between neural tissue and toxic and inflammatory agents inherent in the blood. In all three cases, our model permits real-time monitoring of physiological parameters amenable to fluorescence microscopy (e.g. blood flow, Ca^{2+} dynamics) as well as the three-dimensional localization that is crucial for post-mortem histological and immunological study.

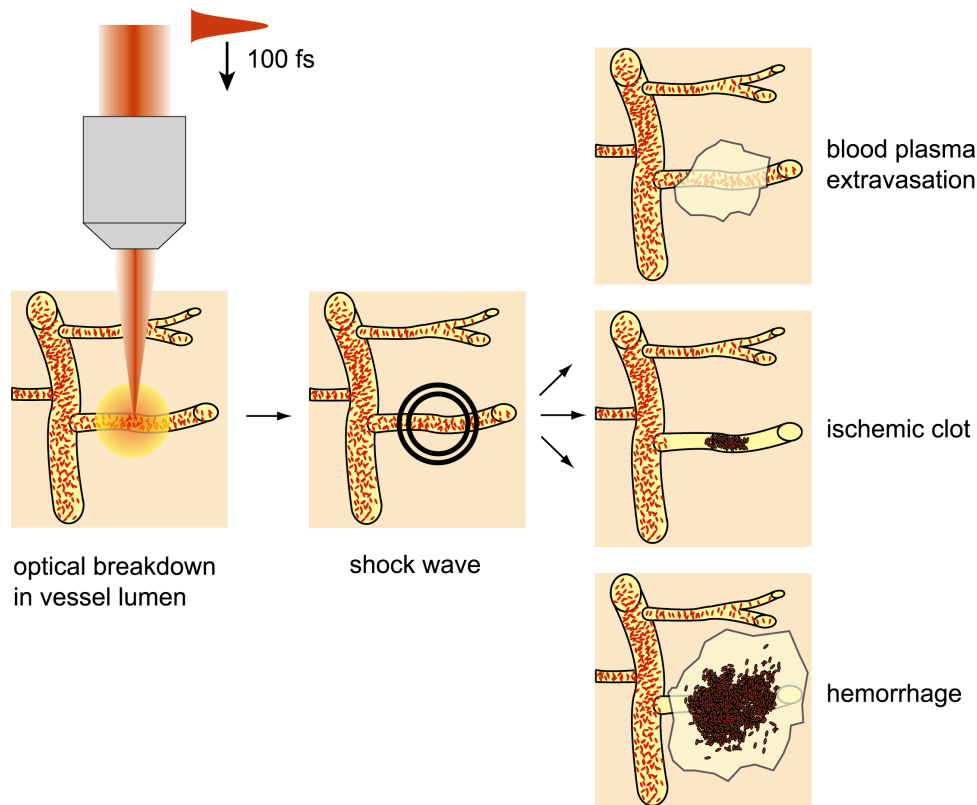


Figure 5. Schematic of the ultrashort laser-induced stroke model. Photodisruption is initiated by the focusing of amplified ultrashort laser pulses into the lumen of the target vessel. Subsequent dynamics result in the formation of three types of vascular injury.

4.1 Mechanism for vascular damage

Ultrashort laser-induced breakdown has been studied extensively. At the focus, nonlinear absorption of high intensity ultrashort laser pulses causes ionization of the material^{20,21}. This is followed by thermodynamic and mechanical effects such as shockwaves and cavitation bubbles²²⁻²⁴. Vascular disruption can be caused by any one of these events. Here, we speculate on the contributions of the various events triggered by irradiation with amplified ultrashort pulses. When the ultrashort laser is focused directly on the vessel wall, ionization removes a portion of the endothelial cell, producing injury. When the laser is focused into the vessel lumen, ionization occurs in blood serum, or perhaps in a passing red blood cell. In this case, the vessel walls are likely not directly affected by the ionization because the ionization volume is small relative to the vessel lumen. However, the shock wave and the cavitation bubble which follow optical breakdown may locally disrupt endothelial cells. The size and strength of the shock wave and cavitation bubble depend on the total amount of laser energy, so that the extent of injury to the vasculature and the tissue can be modulated by the laser power and number of applied pulses.

At low energies, near the threshold for vascular disruption, we posit that a weak shockwave transiently injures the endothelial cells. The injury may be severe enough to degrade the blood brain barrier, allowing the observed extravasation of fluorescein-labeled serum. The injury to the endothelial cells may be sufficiently mild that the cells recover, or the endogenous clotting cascade may seal the breach quickly. The injury can trigger thrombosis that in some cases completely blocks the vessel, but in others leaves the lumen unobstructed. At higher laser energies, we posit that the shockwave may induce sufficient damage to the endothelial cells to disrupt the blood brain barrier for longer times and over larger areas, allowing bodies such as red blood cells to invade the parenchyma. At even higher energies the shockwave and cavitation bubble are thought to be sufficiently strong that they can completely rupture the vessel and possibly induce direct damage to the tissue surrounding the vessels. These larger vascular disruptions result in a hemorrhage that develops into an intra-parenchymal hematoma, a clotted mass that includes red blood cells. We note that even these larger hemorrhages are still three-dimensionally localized, as tissue surrounding the hemorrhage is not disrupted. This tissue immediately bordering these vascular injuries will be at the greatest risk for cell death and consequently, the most interesting to study.

4.2 Significance of the model for clinical research

Current models of stroke are not ideal for the study of distributed, small vascular disruptions that may contribute to neurovascular diseases. Diffuse hemorrhages can be induced by systemic or local injections of agents such as collagenase²⁵ or tissue-plasminogen activator²⁶ to weaken vessels or disrupt the blood brain barrier. Using such models to evaluate potential treatments is difficult because the effects of these agents can be spread over large, uncontrolled regions. In addition, the effects of the agent cannot be isolated to the vasculature and can directly affect the surrounding tissue. Other models use the injection of blood or blood constituents directly into the parenchyma²⁷. While large hematomas can be produced, it is difficult to produce many smaller hemorrhages and this model does not include vascular injury. With our model, vessel ruptures can now be investigated in controlled experiments. Microvessels can be ruptured throughout the cortex to model the microbleeds detected in humans by MRI. There are currently no other models available for studying these small hemorrhages.

Previous models of diffuse ischemic strokes involved the systemic injection of small clotting agents such as microspheres or emboli²⁸⁻³⁰. The locations of the occlusions are random and unpredictable, and infarcts must be located post-mortem by the tedious inspection of the entire brain after histological sectioning. Using our model of intravascular clots, single microvessel occlusions can be placed in a predictable manner deep into the cortex. The subsequent cellular and physiological events can now be systematically studied.

It has not been established that the source of clinically observed lacunar stroke, microinfarcts and vascular dementia is necessarily ischemia, or the cessation of blood flow in a region. Our model of localized blood plasma extravasation may provide insight on a non-ischemic route to localized neuronal death. Several chemicals and proteins in the blood plasma are known to be toxic to neurons. Localized failures in the blood-brain barrier may contribute to neural degeneration. Our model can be used to study the effects of leaking blood plasma and its constituents into the neuronal parenchyma with and without ischemia.

4.3 Alternate methods

Lasers have previously been used to induce stroke or other types of injury in the brain³¹. However, existing techniques are limited to surface damage, often involve the use of photosensitizing molecules in the blood stream, and are often spread over large areas of the brain because much of this work relies on one-photon processes. In our method photodisruption results from the highly nonlinear absorption (via multiphoton and avalanche ionization) of laser energy by material in the focal volume. Because the nonlinear absorption processes require high laser intensities, absorption can be localized to the focal volume of a tightly focused beam of femtosecond laser pulse. Recently, photochemical thrombosis in single cortical vessels has been demonstrated on single vessels,^{32,33} however, because this method also relies on one-photon processes, these occlusions are limited to surface vasculature.

The main advantages of laser-induced vascular disruption are the three-dimensional localization and the control of the affected volume. Laser-induced vascular disruption is a physiologically relevant model because the affected vasculature is in the depth of cortex, surrounded by normal tissue. Unlike systemic models of hemorrhage or ischemia, the interactions between damaged and normal tissue can be studied in a realistic setting. Controlled localization of the vascular disruption allows the identification of the relevant tissues for study of the pathophysiology. In contrast to surface hemorrhages that can be caused by existing surgical techniques, deep photodisruptive hemorrhages bleed directly into the parenchyma. The dynamics of the vascular disruption, clot formation, and hemorrhages are monitored in real-time with TPLSM, allowing us to modify the laser parameters to tailor the types of vascular injuries induced.

ACKNOWLEDGMENTS

This work was supported by the National Institute of Health, the National Institute of Neurological Disorders and Stroke, the National Science Foundation, the Burroughs Wellcome Fund, and the David and Lucille Packard Foundation.

REFERENCES

1. Heye, N. & Cervos-Navarro, J. Microthromboemboli in acute infarcts: analysis of 40 autopsy cases. *Stroke* **27**, 431-4 (1996).
2. Wardlaw, J. M., Sandercock, P. A., Dennis, M. S. & Starr, J. Is breakdown of the blood-brain barrier responsible for lacunar stroke, leukoaraiosis, and dementia? *Stroke* **34**, 806-12 (2003).
3. Pantoni, L. & Garcia, J. H. Pathogenesis of leukoaraiosis: a review. *Stroke* **28**, 652-9 (1997).
4. O'Brien, J. T. et al. Vascular cognitive impairment. *Lancet Neurol* **2**, 89-98 (2003).
5. Lee, S. H. et al. Cerebral microbleeds are regionally associated with intracerebral hemorrhage. *Neurology* **62**, 72-6 (2004).
6. Kidwell, C. S. et al. Magnetic resonance imaging detection of microbleeds before thrombolysis: an emerging application. *Stroke* **33**, 95-8 (2002).
7. Glezer, E. N. et al. Three-dimensional optical storage inside transparent materials. *Optics Letters* **21**, 2023-2025 (1996).
8. Davis, K. M., Miura, K., Sugimoto, N. & Hirao, K. Writing Waveguides in Glass with a Femtosecond Laser. *Optics Letters* **21**, 1729-1731 (1996).
9. Schaffer, C. B., Brodeur, A., Garcia, J. F. & Mazur, E. Micromachining bulk glass by use of femtosecond laser pulses with nanojoule energy. *Optics Letters* **26**, 93-95 (2001).
10. Juhasz, T. et al. Corneal refractive surgery with femtosecond lasers. *IEEE Journal of Selected Topics in Quantum Electronics* **5**, 902-910 (1999).
11. Tirlapur, U. K. & Konig, K. Targeted transfection by femtosecond laser light. *Nature* **418**, 290-291 (2002).
12. Konig, K., Riemann, I. & Fritzsche, W. Nanodissection of human chromosomes with near-infrared femtosecond laser pulses. *Optics Letters* **26**, 819-821 (2001).
13. Tsai, P. S. et al. All-optical histology using ultrashort laser pulses. *Neuron* **39**, 27-41 (2003).
14. Kleinfeld, D., Mitra, P. P., Helmchen, F. & Denk, W. Fluctuations and stimulus-induced changes in blood flow observed in individual capillaries in layers 2 through 4 of rat neocortex. *Proceedings of the National Academy of Sciences USA* **95**, 15741-15746 (1998).
15. Chaigneau, E., Oheim, M., Audinat, E. & Charpak, S. Two-photon imaging of capillary blood flow in olfactory bulb glomeruli. *Proc Natl Acad Sci U S A* **100**, 13081-6 (2003).
16. Denk, W., Strickler, J. H. & Webb, W. W. Two-photon laser scanning fluorescence microscopy. *Science* **248**, 73-76 (1990).
17. Kleinfeld, D. & Denk, W. in *Imaging Neurons: A Laboratory Manual* (eds. Yuste, R., Lanni, F. & Konnerth, A.) 23.1-23.15 (Cold Spring Harbor Laboratory Press, Cold Spring Harbor, 2000).
18. Kleinfeld, D. & Delaney, K. R. Distributed representation of vibrissa movement in the upper layers of somatosensory cortex revealed with voltage sensitive dyes. *Journal of Comparative Neurology* **375**, 89-108 (1996).
19. Backus, S. et al. High-efficiency, single-stage 7-kHz high-average-power ultrafast laser system. *Optics Letters* **26**, 465-467 (2001).
20. Stuart, B. C. et al. Nanosecond-to-subpicosecond laser-induced breakdown in dielectrics. *Physical Review B* **53**, 1749- (1996).
21. Vogel, A. et al. Energy balance of optical breakdown in water at nanosecond to femtosecond time scales. *Applied Physics B-Lasers & Optics* **68**, 271-280 (1999).
22. Noack, J. & Vogel, A. Single-shot spatially resolved characterization of laser-induced shock waves in water. *Applied Optics* **37**, 4092-9 (1998).
23. Schaffer, C. B., Nishimura, N., Glezer, E. N., Kim, A. M. T. & Mazur, E. Dynamics of femtosecond laser-induced breakdown in water from femtoseconds to microseconds. *Optics Express* **10**, 196-203 (2002).
24. Juhasz, T., Kastis, G. A., Suarez, C., Bor, Z. & Bron, W. E. Time-resolved observations of shock waves and cavitation bubbles generated by femtosecond laser pulses in corneal tissue and water. *Lasers Surg Med* **19**, 23-31 (1996).
25. Rosenberg, G. A., Mun-Bryce, S., Wesley, M. & Kornfeld, M. Collagenase-induced intracerebral hemorrhage in rats. *Stroke* **21**, 801-7 (1990).
26. Dijkhuizen, R. M., Asahi, M., Wu, O., Rosen, B. R. & Lo, E. H. Rapid breakdown of microvascular barriers and subsequent hemorrhagic transformation after delayed recombinant tissue plasminogen activator treatment in a rat embolic stroke model. *Stroke* **33**, 2100-4 (2002).
27. Xue, M. & Del Bigio, M. R. Intracortical hemorrhage injury in rats : relationship between blood fractions and brain cell death. *Stroke* **31**, 1721-7 (2000).

28. Overgaard, K. Thrombolytic therapy in experimental embolic stroke. *Cerebrovasc Brain Metab Rev* **6**, 257-86. (1994).
29. Kudo, M., Aoyama, A., Ichimori, S. & Fukunaga, N. An animal model of cerebral infarction. Homologous blood clot emboli in rats. *Stroke* **13**, 505-8. (1982).
30. Krueger, K. & Busch, E. Protocol of a thromboembolic stroke model in the rat: review of the experimental procedure and comparison of models. *Invest Radiol* **37**, 600-8. (2002).
31. Watson, B. D., Dietrich, W. D., Busto, R., Wachtel, M. S. & Ginsberg, M. D. Induction of reproducible brain infarction by photochemically initiated thrombosis. *Annals of Neurology* **17**, 497-504 (1985).
32. Nakase, H., Kakizaki, T., Miyamoto, K., Hiramatsu, K. & Sakaki, T. Use of local cerebral blood flow monitoring to predict brain damage after disturbance to the venous circulation: cortical vein occlusion model by photochemical dye. *Neurosurgery* **37**, 280-5; discussion 285-6 (1995).
33. Schaffer, C. B. et al. in *Commercial and Biomedical Applications of Ultrafast Lasers III* (eds. Neev, J., Ostendorf, A. & Schaffer, C. B.) 222-231 (SPIE- International Society of Optical Engineering, San Jose, 2003).